Research on the Separation and Valorization of Lignocellulosic Components from Distiller's Grains

Siya Liu *, Yimeng Yang

School of Chemistry and Chemical Engineering, Central South University, Changsha, China, 410083

* Corresponding Author Email: 8202220324@csu.edu.cn

Abstract. The high proportion of lignocellulose in distiller's grains plays a significant role in their resource utilization. In this study, the distiller's grains were pretreated, and cellulose, hemicellulose, and lignin were extracted and separated using an ethanol-alkali cooking method. The black liquor obtained after lignin separation was utilized for electrocatalytic hydrogen production, demonstrating high proton transfer efficiency at a relatively low voltage. The extracted cellulose and lignin were characterized by Fourier-transform infrared spectroscopy (FTIR), X-ray diffraction (XRD), and scanning electron microscopy (SEM), confirming their high yield and purity.Throhgh the procedure, this study achieved comprehensive high-value utilization of distiller's grains without secondary pollutants.

Keywords: Distiller's Grains, Lignocellulosic, Ethanol-Alkali Cooking Method, Electrocatalytic Hydrogen Production.

1. Introduction

Distiller's grains, a major byproduct of liquor production, can cause severe ecological pollution if improperly managed [1]. Their high moisture content, acidity, and crude fiber content significantly limit their utilization potential [2]. Therefore, improving the resource efficiency of distiller's grains is an urgent challenge. LIU YH and co-wokers[3] investigate sodium hydroxide pretreatment, step-by-step enzymatic hydrolysis, and simultaneous saccharification and fermentation (SSF) to separate lignocelluloses and residual starch, and then effectively convert distillers' grains to fuel ethanol and other valuable production. Ojo A O[4] Converse lignocellulosic biomass into value-added products by pretreatment, hydrolysis, fermentation,and product purification/recovery .Si M and co-workes[5] designed an acid-catalyzed tetrahydrofuran–water (THF–H 2 O) co-solvent system was designed for the preparation of multiple bio-nanomaterials from natural lignocellulose, including microfibrillated celluloses (MFCs), lignin nanoparticles (LNPs), and carbon quantum dots (CQDs). Choi Y and co-wokers[6] presented a photoelectrochemical cell to extrac electrons from solid lignocellulose biomass by using phosphomolybdic acid as a soluble catalyst and an electron/proton mediator for hydrogen production.

This study aimed to enhance the resource utilization and economic value of distiller's grains by isolating and extracting their valuable components, improving the problems of environmental pollution, high cost and complex operation in the previous research. In this process, both the filtrate and filter residue could be further recycled, with no secondary pollutants generated.

2. Targeted Isolation of the Three Lignocellulose Components: Cellulose, Hemicellulose and Lignin from Distiller's Grains

2.1. Pretreatment of Distiller's Grains

The raw distiller's grains were washed with deionized water to remove residual starch, then dried and homogenized using a blender. The samples were further dried in an oven at 60 °C until constant weight was achieved and stored in the dark to prevent degradation.

Pretreatment is a critical step to reduce biomass recalcitrance, remove inhibitors, and facilitate subsequent fractionation of cellulose, hemicellulose, and lignin.

2.2. Separation and extraction of cellulose and lignin

Ethanol-Alkali Cooking Process: The distiller's grain powder was subjected to ethanol-alkali treatment using 0.5 M NaOH in 25% ethanol aqueous solution at 90°C under continuous magnetic stirring (600 rpm, 4 h). The resulting dark black slurry was then filtered to separate: The filtrate (black liquor), which was collected for subsequent lignin extraction. The solid residue, which contained crude cellulose.

The solid phase was washed thoroughly with distilled water. The washed residue was further treated with a mixed solution containing 22.1 mL nitric acid and 78.9 mL ethanol under reflux conditions for 4 h. After cooling, the mixture was filtered and washed with ethanol. This reflux treatment was repeated twice, during which the solution color progressively changed from brown to pale yellow. The final product was filtered, washed with distilled water, and dried at 60°C to obtain light-yellow cellulose powder.

The liquid phase was heated to 75 °C under continuous magnetic stirring for 1 h, followed by gradual cooling to room temperature. Lignin was precipitated by dropwise addition of 6 M H_2SO_4.The lignin-rich residue was washed and dried at 60 °C for 12 h. The remaining black liquor was collected for subsequent electrocatalytic hydrogen production experiments.

3. Characterization and Analysis of Products

3.1. Characterization and Analysis of Cellulose

3.1.1 Fourier-transform infrared spectroscopy (FTIR) Analysis

The extracted cellulose from distiller's grains was characterized by FTIR spectroscopy using commercial cellulose for reference, as shown in Figure 1.The FTIR spectrum showed distinct absorption peaks at approximately 1500 cm^{-1}, 1730 cm^{-1}, and 2919 cm^{-1}. These characteristic peaks can be assigned as follows:

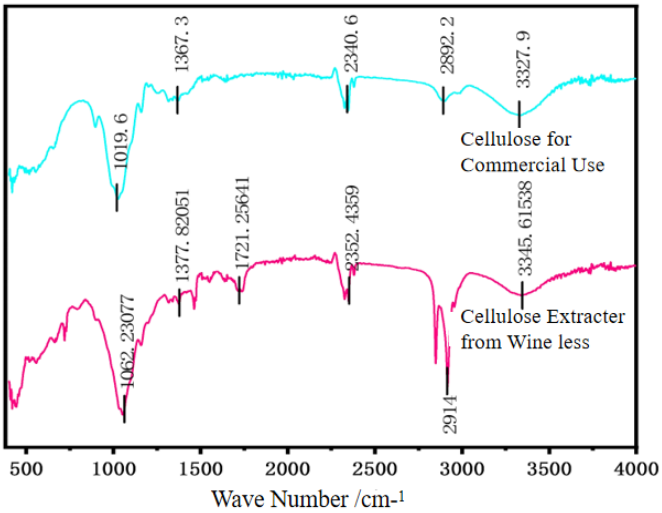

Figure 1. Infrared spectrogram of cellulose

The peak at 2919 cm^{-1} corresponds to C-H stretching vibrations in methyl and methylene groups, which is typical of cellulose's polysaccharide structure.

The absorption at 1730 cm^{-1} indicates the presence of carbonyl (C=O) stretching from acetyl or uronic ester groups, characteristic of residual hemicellulose [6].

The peak near 1500 cm^{-1} represents aromatic ring vibrations (C=C stretching), suggesting trace amounts of residual lignin [7].

In Conclusion, the ethanol-alkali cooking method successfully isolated cellulose from distiller's grains, as evidenced by the dominant cellulose peaks. However, the presence of minor bands at 1730 cm^{-1} (hemicellulose) and 1500–1592 cm^{-1} (lignin) indicates trace residuals.

3.1.2 X-ray Diffraction (XRD) Analysis

The crystallinity of cellulose extracted from distiller's grains was analyzed using X-ray powder diffraction, as shown in Figure 2. The Crystallinity Index (CrI), which reflects the relative proportion of crystalline to amorphous regions in cellulose, was calculated using the Scherrer equation[8], yielding a CrI of 58.10%,which was lower than commercial microcrystalline cellulose (~70–80%). This was due to:efficient removal of hemicellulose and lignin, which partially degraded crystalline cellulose domains during extraction; high protein content in distiller's grains, which, upon dissolution, may have caused cellulose swelling and reduced crystallinity [9]. The results indecated effective delignification and hemicellulose removal.

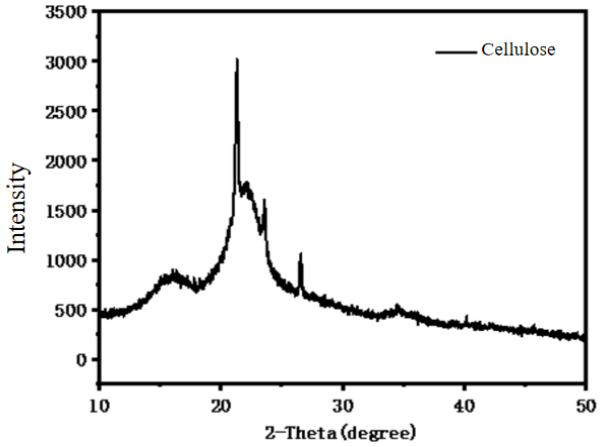

Figure 2. XRD pattern of cellulose

3.1.3 Scanning Electron Microscopy (SEM) Analysis

The surface morphology of cellulose extracted from distiller's grains was examined by SEM, as shown in Figure 3. Structural Characteristics can be observed that it exhibited a loose, porous surface morphology, distinct from compact raw fibers, which was may induced by Ethanol-alkali cooking[10] via protein dissolution and swelling effect. The porous structure provides high surface area for downstream nanofibrillation.

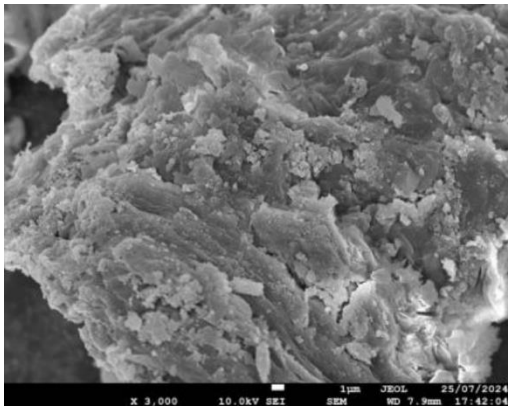

Figure 3. SEM image of cellulose

3.1.4 Cellulose Yield Calculation

The Cellulose Yield (89.17%) was calculated by the following Equation:

$$W_1 = \frac{m_1}{m} \times 100\% \quad (1)$$

Were, m: Mass of crude fiber in raw distiller's grains (g), m_1: Mass of dried purified cellulose (g), W_1: Cellulose yield (%).

3.2. Characterization and Analysis of Lignin

3.2.1 Fourier-transform infrared spectroscopy (FTIR) Analysis

The lignin isolated from distiller's grains was compared with commercial lignin via FTIR spectroscopy, as shown in Figure 4. The spectra exhibited high similarity, confirming successful lignin extraction, with minor deviations attributed to residual polysaccharides: The peak at 2922.1 cm^{-1} corresponds to C-H stretch (alkyl groups), likely from residual hemicellulose (acetyl groups) or cellulose (methylene bridges).

To sum up, The ethanol-alkali method extracted high-purity lignin with minimal cellulose and hemicellulose.

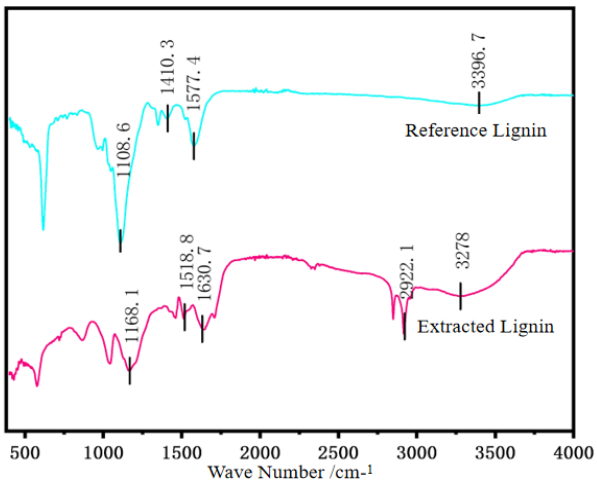

Figure 4. Infrared spectrogram of lignin

3.2.2 X-ray Diffraction (XRD) Analysis

The X-ray diffraction (XRD) pattern of the lignin isolated from distiller's grains confirmed its amorphous nature, consistent with typical lignin structure, as shown in Figure 5.

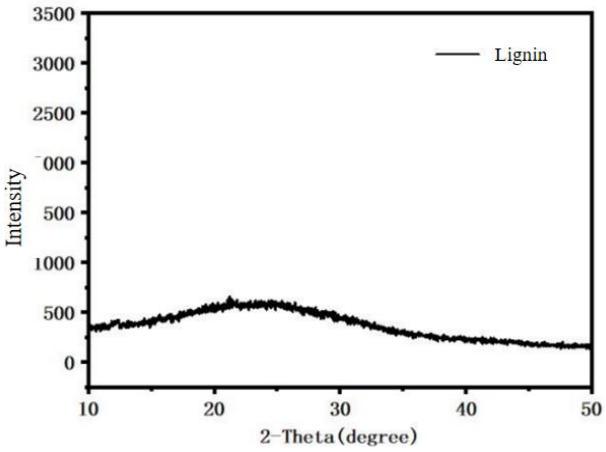

Figure 5. XRD pattern of lignin

3.2.3 Scanning Electron Microscopy (SEM) Analysis

The surface morphology of lignin isolated from distiller's grains was characterized by SEM, as shown in Figure 6, revealing highly porous surface and rough texture, which leaded to preferable adsorption capacity.

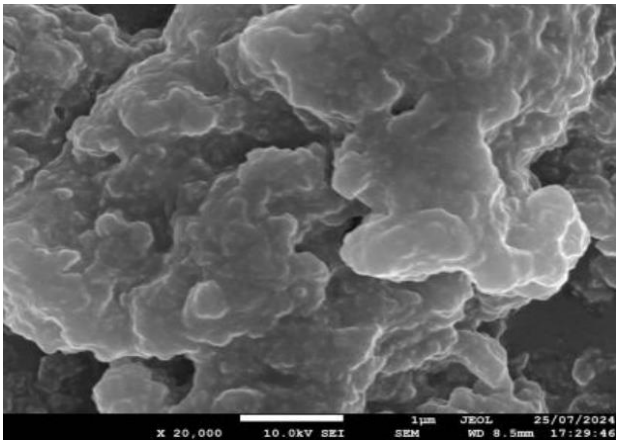

Figure 6. SEM pattern of lignin

3.2.4 Lignin Yield Calculation

The Lignin Yield (89.17%) was calculated by the following Equation:

$$W_2 = \frac{m_2}{m} \times 100\% \quad (2)$$

Were, m: Mass of crude fiber in raw distiller's grains (g), m_2: Mass of dried purified lignin (g), W_2: lignin yield (%).

4. Black Liquor Electrolysis for Hydrogen Production

4.1. Experimental Procedure for Efficient Hydrogen Generation

4.1.1 Redox Reaction Between Black Liquor and Phosphomolybdic Acid

5.48 g of PMA ($H_3PMo_{12}O_{40}$) was dissolved in 10 mL deionized water, forming a yellow suspension. Then it was heated at 100 °C under magnetic stirring (300 rpm) until a transparent yellow solution was obtained.10 mL of black liquor was added to the PMA solution. The mixture was stirred at 100 °C for 6 h, during which the solution gradually turned deep blue, indicating $Mo^{6+} \rightarrow Mo^{5+}$ reduction by hemicellulose-derived aldehyde compounds.

4.1.2 Electrocatalytic Hydrogen Production

System Configuration, as shown in Figure 7: Anolyte was attached to post-reaction black liquor-PMA solution (containing reduced Mo^{5+}/Mo^{4+}). Catholyte was attached to 1 M H_3PO_4 aqueous solution (proton source). The two electrodes were connected by flow cell configuration. Electrolysis and I-V Testing took place in the flow cell system.

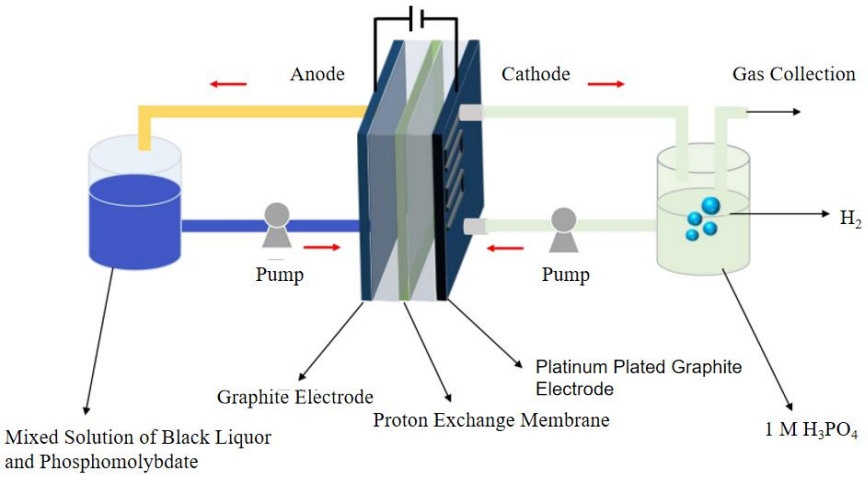

Figure 7. Schematic diagram of black liquor hydrogen electrolysis device

Anode (Oxidation):

$$Mo^{5+} \rightarrow Mo^{6+} + e^{-} \quad (3)$$

Cathode (Reduction):

$$2H^{+} + 2e^{-} \rightarrow H_2 \uparrow \quad (4)$$

Net Reaction:

$$\text{Reduced molybdenum} + 2H^{+} \rightarrow \text{Molybdenum oxide} + H_2 \uparrow \quad (5)$$

4.2. Analysis of Efficient Hydrogen Production from Black Liquor

1. Low-voltage hydrogen production performance,as shown in Figure 8

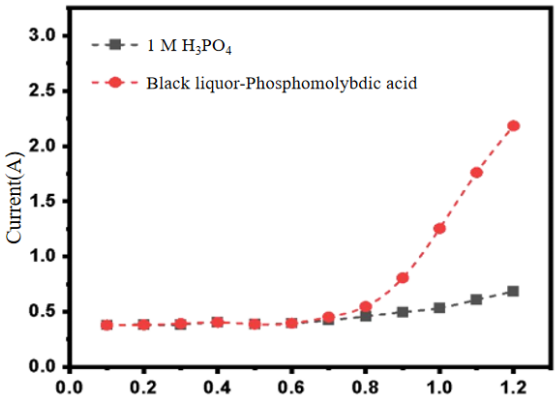

Figure 8. Black liquor - phosphomolybdate solution I-V test spectrum

When the applied voltage exceeded 0.8 V, the current density increased sharply with simultaneous hydrogen evolution observed at the cathode. This onset potential is significantly lower than that required for water electrolysis (1.23 V), demonstrating the system's capability for efficient hydrogen production at reduced voltage with substantially lower energy consumption.

2. Galvanostatic electrolysis experiment, as shown in Figure 9

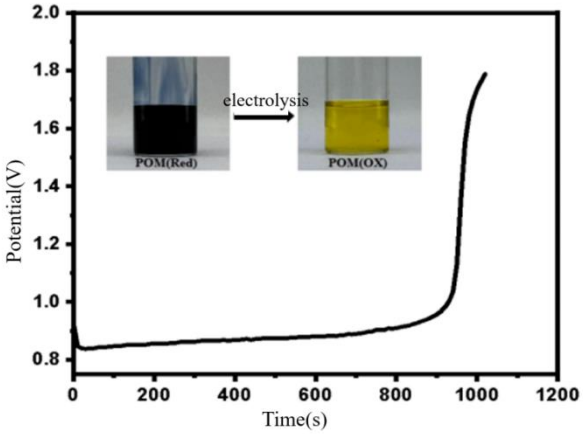

Figure 9. Hydrogen production by electrolysis of black liquor-phosphomolybdate solution

Using a constant current density of 100 mA/cm², the mixed solution of 10 mL black liquor reacted with 0.3 M phosphomolybdic acid for 6 hours was electrolyzed. After 15 minutes, the solution color transitioned completely from deep blue (Mo^{5+}) to transparent yellow (Mo^{6+}), marking the completion of the first electrolysis cycle, during which 10.4 mL of hydrogen gas was collected.

3. Faradaic efficiency analysis,as shown in Figure 10,Figure 11

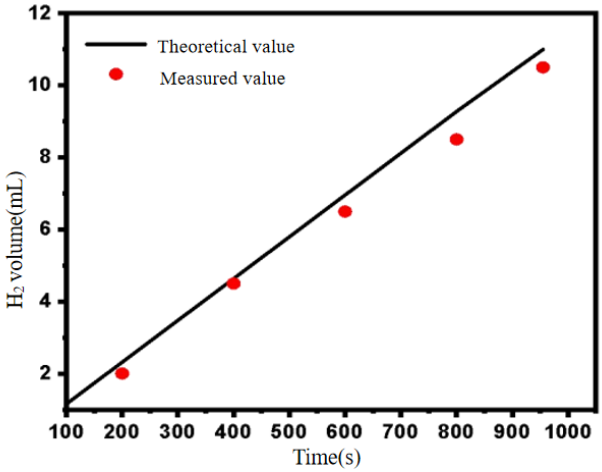

Figure 10. The volume of hydrogen collected and the theoretical value at different times in the electrolysis process

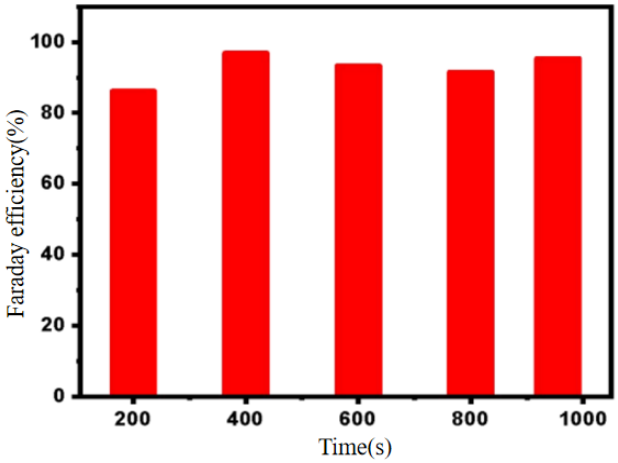

Figure 11. Faraday efficiency calculated at different times

Comparison between the theoretically calculated hydrogen volume (via Faraday's law) and actually collected volume yielded a Faradaic efficiency of 92.7%, indicating exceptionally efficient proton transfer in the system.

5. Conclusions

There is gerat valorization potential of distiller's grains. This study developed an integrated and environmentally benign biorefinery platform for efficient valorization of distiller's grains. High-purity cellulose and lignin were successfully extracted with remarkable yields of 89.17% and 95.04% respectively, as confirmed by comprehensive characterization analyses (FTIR, XRD, SEM), thereby establishing a crucial foundation for their downstream high-value applications. The innovative utilization of waste liquor for hydrogen production via thermochemical-electrochemical hybrid electrolysis demonstrated superior energy efficiency, reducing energy consumption by >50% compared to conventional water electrolysis.

The complete valorization approach achieved: Maximum resource recovery through full-component utilization, Near-zero waste generation with closed-loop processing, Significant energy savings in hydrogen production, High-quality intermediates ready for value-added conversion. The experimental procedure demonstrated both environmental friendliness and operational simplicity. Moreover, the resulting products exhibited broad application potential and significant market demand. Consequently, this approach holds promise for scalable industrial production.

References

[1] De Iseppia A, Lomolino G, Marangon M, et al. Current and future strategies for wine yeast lees valorization[J]. Food Research International, 2020, 137: 109352.

[2] Mei S H, Zhu M M, Wang W, et al. Study on solid-state fermentation conditions of Baijiu distillers' grains by compound probiotics[J]. Chinese Journal of Animal Nutrition, 2023, 35(1): 632-642. (in Chinese)

[3] Liu Y H, Wu Z Y, Yang J, et al. Step enzymatic hydrolysis of sodium hydroxide-pretreated Chinese liquor distillers' grains for ethanol production[J]. Preparative Biochemistry and Biotechnology, 2014, 44(5): 464-479.

[4] Ojo A O. An overview of lignocellulose and its biotechnological importance in high-value product production[J]. Fermentation, 2023, 9(11): 990.

[5] Si M, Sillanpää M, Zhuo S, et al. Phase separation of co-solvent promotes multiple bio-nanomaterials conversion from natural lignocellulose[J]. Industrial Crops and Products, 2020, 152: 112469.

[6] Choi Y, Mehrotra R, Lee S H, et al. Bias-free solar hydrogen production at 19.8 mA cm−2 using perovskite photocathode and lignocellulosic biomass[J]. Nature Communications, 2022, 13(1): 5709.

[7] Ilyas R A, Sapuan S M, Ishak M R. Isolation and characterization of nanocrystalline cellulose from sugar palm fibres (Arenga Pinnata) [J]. Carbohydrate Polymers, 2018, 181: 1038-1051.

[8] Anass A B, Zineb K, Abdelghani B, et al. Beneficiation of cactus fruit waste seeds for the production of cellulose nanostructures: Extraction and properties[J]. International Journal of Biological Macromolecules, 2022, 203: 302-311.

[9] Yang X. Pretreatment of lignocellulose with p-toluenesulfonic acid and its comprehensive utilization[D]. Beijing University of Chemical Technology, 2020. (In Chinese)

[10] Li C. Preparation and application of lignin-based carbon nanomaterials based on DES pretreatment[D]. Beijing University of Chemical Technology, 2022. (In Chinese)